NASA TECHNICAL NOTE

NASA TN D-3237

NASA TN D-3237

THERMAL NEUTRON FLUX PERTURBATION BY DYSPROSIUM-ALUMINUM FOILS IN WATER AND URANYL FLUORIDE - WATER SOLUTIONS

by Donald F. Shook, Donald Bogart, Donald L. Alger,
and Robert A. Mueller

Lewis Research Center
Cleveland, Ohio

NATIONAL AERONAUTICS AND SPACE ADMINISTRATION • WASHINGTON, D. C. • MARCH 1966

NASA TN D-3237

THERMAL NEUTRON FLUX PERTURBATION BY DYSPROSIUM-ALUMINUM FOILS IN WATER AND URANYL FLUORIDE - WATER SOLUTIONS

By Donald F. Shook, Donald Bogart, Donald L. Alger,
and Robert A. Mueller

Lewis Research Center
Cleveland, Ohio

NATIONAL AERONAUTICS AND SPACE ADMINISTRATION

For sale by the Clearinghouse for Federal Scientific and Technical Information
Springfield, Virginia 22151 – Price $1.00

THERMAL NEUTRON FLUX PERTURBATION BY DYSPROSIUM-ALUMINUM FOILS IN WATER AND URANYL FLUORIDE - WATER SOLUTIONS

by Donald F. Shook, Donald Bogart, Donald L. Alger, and Robert A. Mueller

Lewis Research Center

SUMMARY

Thermal neutron flux perturbation factors have been measured for dysprosium-aluminum alloy foils in water and uranyl fluoride - water solutions. The foils are representative of a type widely used for thermal neutron flux surveys. The measurements provide additional data for comparison with analytical calculations of foil perturbation factors in water. The uranyl fluoride - water solutions used comprise absorptive diffusion media different from water or graphite that have been studied exclusively in the past. The edges of the thicker dysprosium-aluminum foils used are a significant part of the total foil surface so that the data provide a test for several proposed edge corrections to perturbation factor calculations. The experimental perturbation factors are in good agreement with the predictions of published calculational methods except for the dimensionless generalization of Dalton and Osborn.

INTRODUCTION

The thermal neutron capture rate in foils of practical thickness relative to the capture rate in extremely thin foils having no neutron flux perturbation is required in measurements utilizing foil techniques to determine neutron flux, isotope production rates, or radiation counter efficiency. Because of the importance of specifying the thermal flux perturbation in interpreting foil activation data, the problem has received wide experimental and analytical attention as summarized in references 1 and 2. Most of the measurements of foil perturbation factors to date have been made with thin foils of gold or indium because these materials have been used frequently for flux measurements. The present study extends the range of foil composition and size and the range of diffusion media for which perturbation factors have been measured. The experimental results provide additional tests of calculational methods that consider hardened thermal spectra in the diffusion media and edge effects for thick foils.

The measurements were made with dysprosium-aluminum alloy foils 2.54 centimeters in diameter and stacked up to 0.32 centimeter in thickness so that the edges of the foils are a significant part of the total surface. Since the alloy is largely aluminum (5 percent dysprosium by weight), the range of foil thickness in absorption mean free paths is similar to that for previous measurements using thin gold and indium. The foil activations were made in pure water containing two neutron sources and also in a small homogeneous reactor at several different uranyl fluoride - water concentrations. A comparison of the data for the various media provides a measure of the effects of spectral hardening on foil perturbation factors. These hardening effects enter the analytical evaluation of foil perturbation factors through the spectrally averaged parameters for each media. The basic analytic method of Ritchie and Eldridge (ref. 3) has been employed.

A comparison of experimental perturbation factors for indium foils in water with the factors calculated by the Ritchie and Eldridge method using the edge corrections of Tittle (ref. 4) is presented by Walker et al. (ref. 5).

Foil perturbation factors have also been calculated by monoenergetic transport theory solved iteratively by Dalton and Osborn (ref. 6) for the case of a cylindrical detector in a diffusion medium. For convenience in using the digital computer, the geometry was specialized to right circular cylinders so as to include wire and coin-shaped detectors. Numerical results for water and graphite by Dalton and Osborn are in good agreement with the experimental results for gold foils in water as measured by Zobel (ref. 7). These numerical results were generalized by Dalton and Osborn and presented graphically as dimensionless functions of the foil thickness and foil radius in absorption mean free paths. However, on comparison with perturbation factors calculated by the Ritchie and Eldridge method, this dimensionless generalization is found to be approximately correct for gold and indium but invalid for dysprosium-aluminum.

SYMBOLS

E_3	third order exponential integral
g	neutron flux depression function
L	thermal neutron diffusion length
r	radius
S/V	ratio of surface area to volume
t	thickness
α	$1 - 2E_3(\tau)$
γ	Σ_S/Σ_T
ϵ	edge correction
λ	total neutron mean free path
λ_S	scattering mean free path
λ_{tr}	transport mean free path

$\bar{\mu}$	average value of cosine of neutron-scattering angle
Σ_a	macroscopic neutron absorption cross section
Σ_S	macroscopic neutron scattering cross section
Σ_T	total macroscopic cross section
τ	thickness in neutron mean free paths
τ_0	thickness in mean free paths evaluated at neutron energy of 0.025 eV

ANALYSIS

The various theoretical analyses that have led to expressions for the neutron flux perturbation due to a finite absorbing foil in a thermalizing diffusion medium have been reviewed recently by Osborn (ref. 1). Comparisons of the analytical predictions of foil perturbation factors with the available experimental results for graphite and hydrogenous media have been presented by Hanna (ref. 2). The difficulties of analyzing the complex spatial and polyenergetic problem have led to the use of approximate perturbation factors. Spectrum-averaged parameters have been used in monoenergetic transport analysis in an effort to take care of the unique equilibrium thermal spectrum that exists in the diffusing medium surrounding the finite absorbing foil.

The foil perturbation factor F is defined as the ratio of the foil capture rate in the perturbed flux to that which would result in an unperturbed flux. The perturbation factor depends on the average neutron scattering and absorption properties of the diffusion medium as well as on the size and average capture and scattering cross sections of the foil. In the notation of Hanna (ref. 2), the expression for F can be written in the general form

$$F = \frac{\frac{\alpha}{2\tau}(1 + \epsilon)}{1 + \frac{\alpha}{2} g} \tag{1}$$

The factor $\alpha/2\tau$ accounts for self-shielding of the incident neutrons within the volume of the foil. For an isotropic neutron flux this quantity is given by

$$\frac{\alpha}{2\tau} = \frac{1 - 2E_3(\tau)}{2\tau}$$

where E_3 is the third order exponential integral. The quantity $\alpha/2\tau$ also corresponds by a reciprocity condition to the escape probability for a uniformly distributed isotropic source in a slab of thickness τ absorption mean free paths and of infinite transverse extent as derived and tabulated by Case et al. (ref. 8).

The factor $1 + \epsilon$ in equation (1) represents an edge correction for foils of finite radius. Edge corrections have been suggested by Hanna (ref. 2) and by Tittle (ref. 4), respectively, as follows:

$$1 + \epsilon_H = 1 + \frac{2\tau}{\alpha}\frac{t}{\pi r}\left(1 - \frac{\pi\tau}{6}\right) \tag{2}$$

$$1 + \epsilon_T = 1 + \frac{t}{2r} \tag{3}$$

The physical basis for these corrections is given in the derivation in reference 2. A third form is suggested herein. Based on the observed correlation between escape probability and the surface to volume ratio (S/V) for bodies of different shapes as computed in reference 8, an edge correction can be formulated from the ratio of (S/V) for a finite disk of radius r and thickness t to that of a disk of the same thickness but of infinite radius $(S/V)_\infty$ as

$$\frac{(S/V)}{(S/V)_\infty} = \frac{\frac{2}{t}\left(1 + \frac{t}{r}\right)}{\frac{2}{t}} = \left(1 + \frac{t}{r}\right) \tag{4}$$

In applying this edge correction, the quantity $1 + \epsilon$ in expression (1) is set equal to unity and equation (4) is employed to reduce the thickness of a finite radius foil to a corrected value τ_{corr} corresponding to τ of an equivalent infinite slab such that

$$\tau_{corr} = \frac{\tau}{1 + \frac{t}{r}}$$

The corrected value τ_{corr} is then used to compute $\alpha/2\tau$ and α in equation (1).

The denominator of equation (1) accounts for the neutron flux depression in the diffusion medium surrounding the finite foil and is a nonseparable function of the properties of the diffusion medium and those of the foil. The expression used here is that of Ritchie and Eldridge (ref. 3) who have made a variational transport theory calculation of $g(\gamma,\tau)_{RE}$ for disks of infinite radii in the diffusion medium. The properties of the diffusion medium are contained in the quantity $\gamma = \Sigma_S/\Sigma_T$ where $\Sigma_T = \Sigma_S + \Sigma_a$ and Σ_a and Σ_S are the macroscopic absorption and scattering cross sections of the medium. Ritchie and Eldridge suggest the use of the transport theory results as a correction to those of Skyrme (ref. 9) who derived an analytical expression for a very thin finite foil which was replaced by a localized capture distribution within the diffusion medium. The expression for the Skyrme g-function as modified by Ritchie and Eldridge is

$$\left[g(\gamma,\tau,r)\right]_S = \frac{3L}{2\lambda} S\left(\frac{2r}{L}\right) - K\left(\frac{2r}{\lambda}, \gamma\right) \tag{5}$$

where L is the thermal neutron diffusion length in the medium, λ is the total mean free path in the medium, and r is the radius of the foil.

The Ritchie-Eldridge g-function is then

$$[g(\gamma,\tau,r)]_{RE} = [g(\gamma,\tau,r)]_S \frac{[g_\infty(\gamma,\tau)]_{RE}}{[g_\infty(\gamma,\tau)]_S} \tag{6}$$

The Skyrme functions S and K of equation (5) as well as the ratio of the infinite foil g-functions of equation (6) are presented graphically in reference 3.

The analytical methods that have been discussed have considered scattering in the surrounding medium to be isotropic in the laboratory system; however, scattering in a lightweight moderating media is actually anisotropic. The effects of flux anistropy have recently been discussed by Walker (ref. 10). In the hydrogenous media of the present experiments, an average value of hydrogen transport mean free path λ_{TR} was used based on

$$\lambda_{TR} = \frac{\lambda_S}{1 - \bar{\mu}} \qquad \bar{\mu} = 0.3$$

where λ_S is the scattering mean free path and $\bar{\mu}$ is the average value of the cosine of the scattering angle.

Inasmuch as the transport theory analyses are monoenergetic and are to be applied to equilibrium thermal flux spectra in the diffusion medium containing the foil, the spectrum dependent variables in equation (1) must be replaced by effective values averaged over the thermal flux spectra in each media. Therefore, the parameters in equation (1) are averaged over the known unperturbed flux spectrum neglecting any effects the presence of the foil may have on the local flux spectra. Averaging procedures have been discussed previously (refs. 3 and 4); the procedures used for the hardened spectra associated with the uranyl fluoride - water solutions and pure water employed in the present experiments are discussed in the section PERTURBATION FACTOR CALCULATIONS.

EXPERIMENT

Foil perturbation factors were determined by measuring the relative activity of foils for a wide range of thicknesses. Perturbation factors in the diffusion medium are obtained as ratios of measured activities to the extrapolated unperturbed foil activity. The same method has been used by Zobel (ref. 7). In the present experiments, measurements for foils in the uranyl fluoride - water solutions were made in an unreflected homogeneous reactor designated NASA ZPR-1. The reactor vessel shown in figure 1 is a cylinder 30.5 centimeters in diameter and 76.2 centimeters high with easy access to the reactor core. The fuel solutions contained uranium isotropically enriched to 93 percent uranium-235; concentrations of uranyl fluoride varied from 6 to 20 percent by weight with corresponding hydrogen-to-uranium-235 atom ratios that varied from 560 to 190. Foils were suspended and irradiated at the center of the reactor by means of the wire holder shown in figure 1. The foil sample was separated from the fuel solution by a 0.0076-centimeter-thick teflon tape. Cadmium-covered foil measurements were made in the same manner using a 0.089-centimeter wall thickness cadmium box contained in a thin-wall lucite container.

Additional measurements were made in a 1.83-meter-diameter by 1.53-meter-high water-filled tank containing neutron sources and a foil holder, as shown in figure 2. Two 5-curie plutonium-beryllium sources were positioned 18 centimeters apart by the lucite holder. Foils were positioned in a thin-walled lucite holder containing a cavity 2.60 centimeters in diameter and 0.16 centimeter high midway between the sources. Demineralized water was used and recirculated through a demineralizer so as to maintain a resistivity of 0.1 megohm.

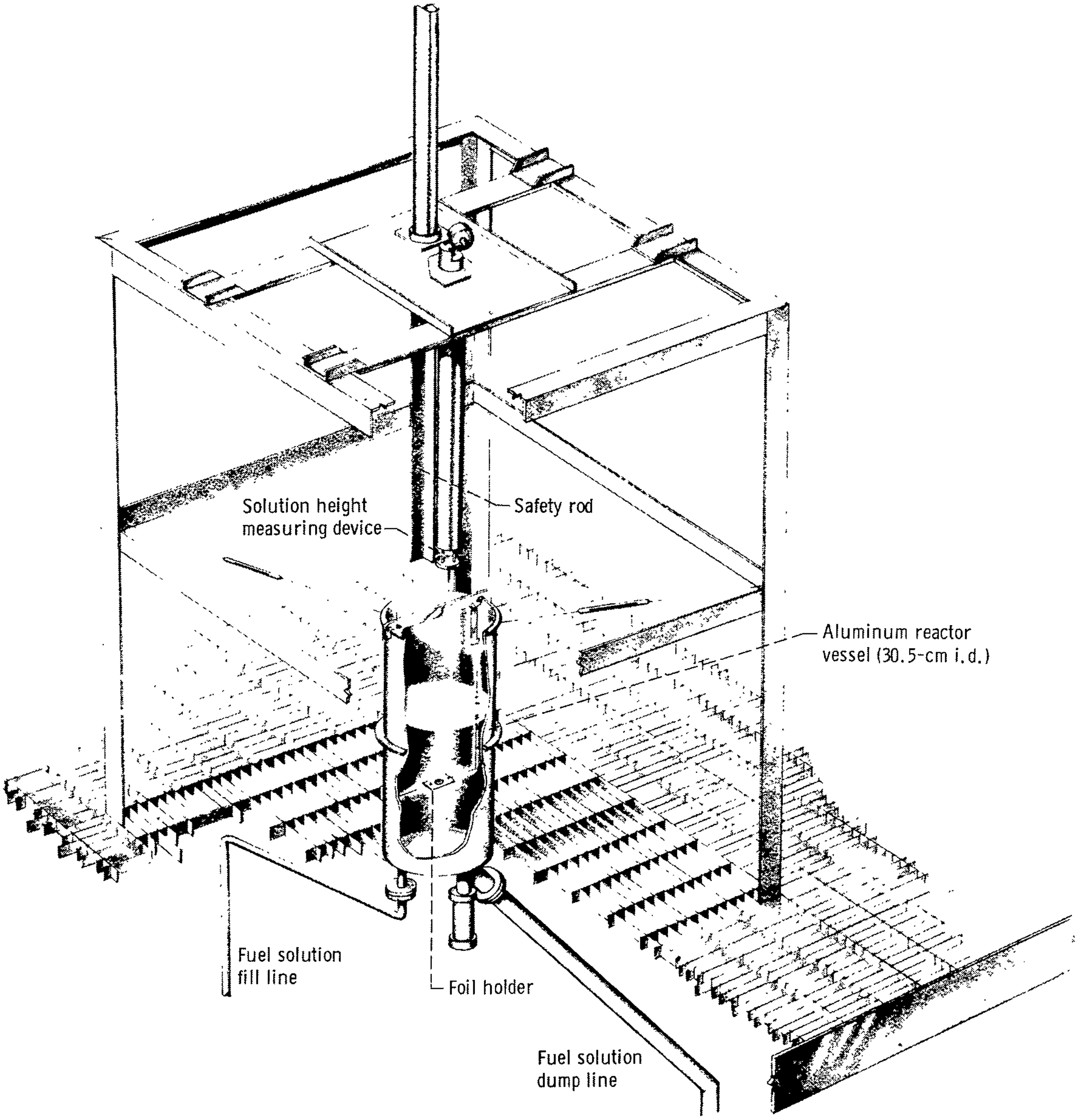

Figure 1. - NASA ZPR I containing uranyl fluoride - water fuel solutions.

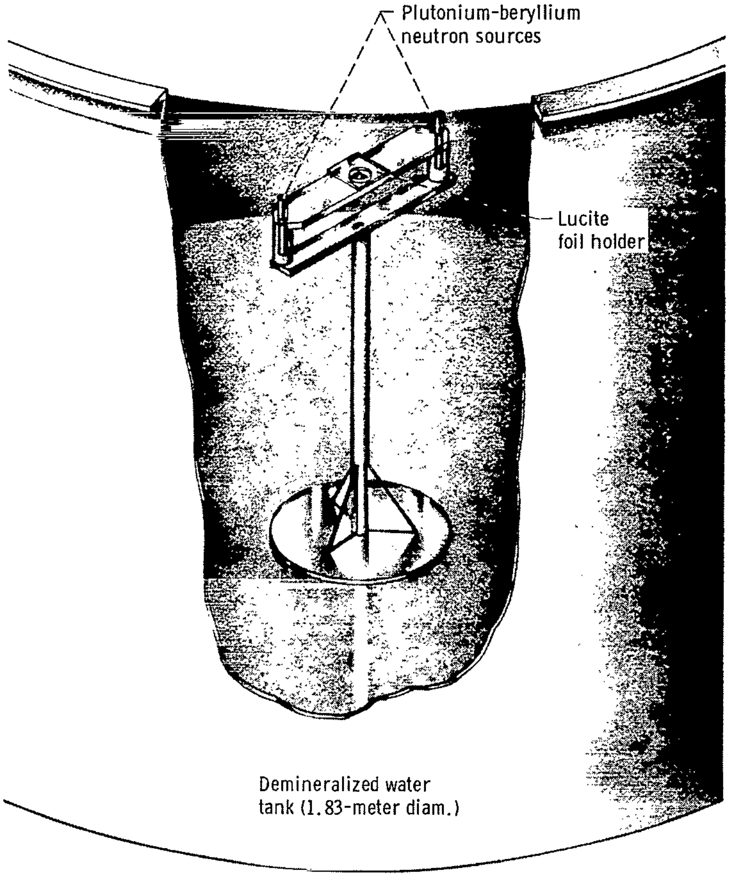

Figure 2. - Water tank containing foil holder and neutron sources.

COUNTING METHOD AND FOIL MASS DETERMINATION

The foils used were made of 0.0127-centimeter-thick dysprosium-aluminum alloy containing 5-percent dysprosium by weight and were 2.56 centimeters in diameter. Foils of various thicknesses were obtained by stacking as many as 19 of the 0.0127-centimeter foils together. The foils were counted individually by using 2π proportional counters except for a few measurements for which the 1.1-million-electron-volt gamma rays of dysprosium-165 were also counted with foils placed in a standard position 10 centimeters from a 5.08-centimeter by 5.08-centimeter sodium iodide crystal using conventional pulse counting equipment. Standard methods of decay correction were used. Proportional counter plateaus were maintained to better than 1 percent per 100 volts, and the counting efficiency varied less than 1 percent for distances up to 1.27 centimeters from the axis of the counting chamber.

The set of twenty 0.0127-centimeter foils were intercalibrated by simultaneous activation on a rotating wheel exposed to a thermal neutron flux. Beta-particle and gamma-ray count rates were measured, and the differences in relative count rates between foils were less than 3 percent. The relative

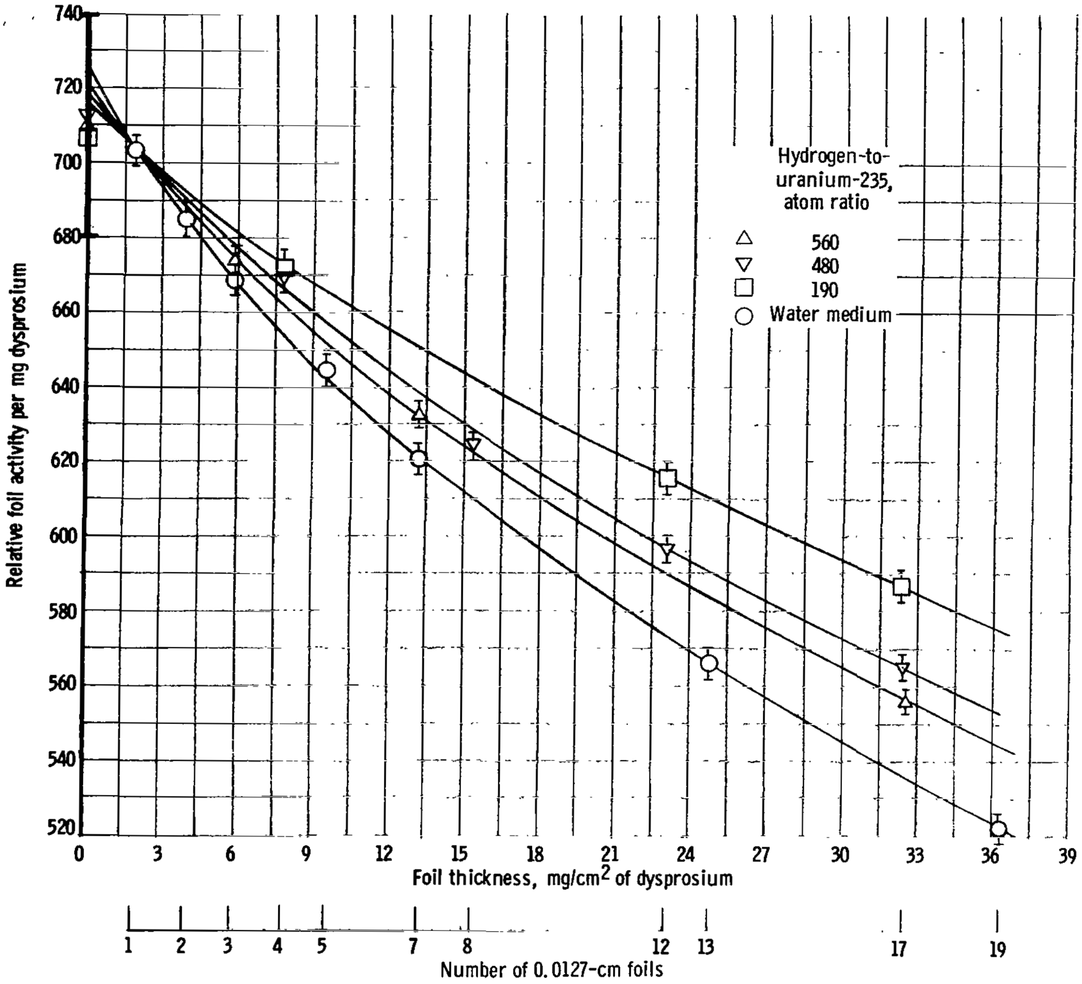

Figure 3. - Dysprosium-aluminum foil activities relative to activity of single 0.0127-centimeter dysprosium-aluminum in water and in uranyl fluoride - water solutions.

count rates of the 1.1-million-electron-volt gamma rays from dysprosium-165 agreed with the relative beta counts, which indicated the relative beta count rates to be insensitive to any thickness variations across the foils. The mass of dysprosium in each foil was obtained as the mass of dysprosium of the standard foil per unit activity times the activity of the foil. The dysprosium mass of the standard foil was obtained by chemical analysis and agreed with that specified by the foil supplier within an estimated uncertainty of 2 percent.

In an attempt to approach the activity per unit mass at zero foil thickness with greater precision, a number of foils containing one-tenth the dysprosium mass of the alloy foils were made by vacuum evaporation of dysprosium on aluminum 0.00254 centimeter thick. Masses were determinad by weighing under controlled conditions since the dysprosium oxidizes and takes on moisture (ref. 11). These foils were activated and the relative gamma-ray activities per milligram of dysprosium were determined.

The subcadmium count rate data for all foils are plotted against foil thickness in milligrams per square centimeter in figure 3; a scale of number of foils is included. The count rates per unit mass are shown normalized to a single 0.0127-centimeter foil. Cadmium-covered foil activities have been subtracted from the data. Cadmium ratios were of the order of 100. The foil thickness of the stacked foils was found to average about 0.0152 centimeter per foil due to spaces between the foils. The error bars on the alloy foil data represent the standard deviation of the foil activities and that of the calibrations used to obtain the relative dysprosium content. For the data on the uranyl fluoride - water solutions, an additional uncertainty is included due to the statistics of the dysprosium foil activities used to monitor reactor power.

The curves in figure 3 are drawn through the data and extrapolated to zero foil thickness. These curves are used to obtain the foil perturbation factors for the various diffusion media. The vapor-plated foil data are used to define an upper bound of uncertainty for the zero thickness foil activity. The rather large uncertainty in the very thin vapor-plated foil data is due primarily to the uncertainty in the measured foil masses.

PERTURBATION FACTOR CALCULATIONS

Equation (1) was employed to calculate foil perturbation factors for water and for the uranyl fluoride - water solutions used. The required parameters representing flux-weighted cross sections from zero to 0.5 electron volt are presented in table I. The parameters $\bar{\Sigma}_S$, $\bar{\Sigma}_a$, $\bar{\tau}$, and $(\bar{\alpha}/2\bar{\tau})$ were obtained by averaging over the measured spectra in equivalently absorptive boron-water solutions of reference 12. The value of τ evaluated at 0.025 electron volt is τ_0. These parameters are generalized in terms of barns of absorber atom per hydrogen atom of moderator in order to obtain average parameter values for a particular uranyl fluoride - water solution. The diffusion length L for hardened thermal spectra were obtained from the experimental boron-water data of reference 13. The escape probability $(\bar{\alpha}/2\bar{\tau})$ was spectrum averaged rather than averaging α and τ separately as performed in reference 4. For consistency, the value of $\bar{\alpha}$ used in the denominator of equation (1) was obtained as $(\bar{\alpha}/2\bar{\tau})2\bar{\tau}$. This method is believed to be more accurate because the uncertainty in F varies directly with $(\bar{\alpha}/2\bar{\tau})$ but varies more slowly with $\bar{\alpha}$ for small values of τ_0.

Also included in table I are values of $(\alpha/2\tau)$ at 0.025 electron volt that are seen to be good approximations to the room temperature water spectrum averaged values when τ_0 is less than 0.3. This had been pointed out previously by Hanna (ref. 2) and by Tittle (ref. 4) for the case of a Maxwellian thermal neutron flux. This approximate procedure could be extended to the uranyl fluoride - water solutions by treating the flux spectra as Maxwellians at elevated temperatures but with a loss in accuracy since the hardened thermal spectra are not Maxwellian.

The parameters in table I are derived for a foil of absorption cross section that varies as the reciprocal of the neutron velocity $1/v$, because of their more general utility. However, dysprosium-164 that accounts for about

TABLE I. - ROOM-TEMPERATURE FLUX-WEIGHTED CROSS SECTIONS

FROM 0 TO 0.5 ELECTRON VOLT

(a) Diffusion medium parameters

Diffusion medium parameter	Diffusion medium			
	Water	Hydrogen-to-uranium-235 atom ratio		
		560	480	190
Barns/H atom	0.33	1.55	1.75	4.92
Average macroscopic scattering cross section, $\bar{\Sigma}$, cm^{-1}	3.10	2.91	2.89	2.70
Average macroscopic absorption cross section, $\bar{\Sigma}_a$, cm^{-1}	0.0190	0.0850	0.096	0.183
Thermal neutron diffusion length, L, cm	2.75	1.26	1.18	0.78
Unit 1 barn cross section at 0.025 eV, 1/v	0.860	0.805	0.790	0.700

(b) Foil capture probability

Foil thickness, τ_0	Neutron spectra				
	Monoenergetic (0.025 eV)	Water	Hydrogen-to-uranium-235 atom ratio		
			560	480	190
	Foil capture parameter, $\alpha/2\tau$				
0.01	0.975	0.976	0.978	0.978	0.981
.03	.935	.943	.947	.948	.953
.05	.902	.915	.922	.923	.930
.08	.862	.880	.889	.891	.900
.10	.827	.859	.870	.872	.883
.30	.665	.709	.728	.732	.753

80 percent of the natural dysprosium capture cross section is known to be non-1/v (ref. 14). The importance of this deviation from 1/v to the present experiments was investigated by flux weighting the absorption probability and foil capture cross sections using the available dysprosium cross section (refs. 14 and 15). For $\tau_0 = 0.3$ and the flux spectra for hydrogen-to-uranium-235 atom ratio of 190, the parameters τ and $(\bar{\alpha}/2\bar{\tau})$ for dysprosium were not significantly different from those for a 1/v cross section. For harder spectra than this or for thicker foils, neutron capture rates at neutron energies between 0.2 and 0.5 electron volt are important. In this region dysprosium sections are non-1/v and resulting parameters differ from those for a 1/v cross section. Under these conditions, perturbation calculations should be made utilizing the actual dysprosium cross sections and an additional spec-

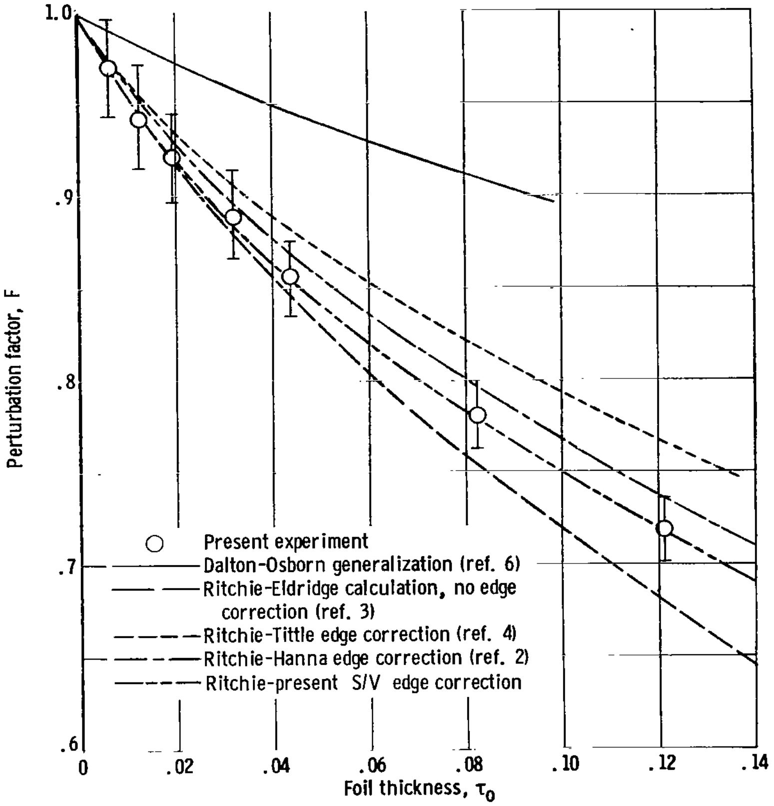

Figure 4. - Foil perturbation factors for 2.54-centimeter-diameter dysprosium-aluminum foils in water.

trum dependent factor. This factor arises because the capture cross section of the isotopes other than dysprosium-164 is probably 1/v; accordingly, a saturated foil activity due to dysprosium-165 is not proportional to the total neutron capture rate.

RESULTS AND DISCUSSION

The perturbation factors obtained from foil activations made in pure water containing two neutron sources and in a small homogeneous reactor at several different uranyl fluoride - water concentrations are presented. The experimental data for water are compared with various calculated curves in figure 4. The dysprosium foil perturbation factors corresponding to each data point of figure 3 are shown. The indicated uncertainty in the perturbation factors reflects primarily the estimated uncertainty in the extrapolation to zero foil thickness indicated in figure 3. The foil optical thickness used in figure 4 is τ_0, the macroscopic absorption cross section times the thickness using $\sigma_{(0.025\ \mathrm{eV})} = 950\pm50$ barns; this uncertainty is the principal contributor to the uncertainty in thickness but is not indicated in the figure for clarity.

Edge Effects

The edges of the thicker dysprosium-aluminum foils used comprise about

TABLE II. - FLUX PERTURBATION FACTORS 2.54-CENTIMETER-DIAMETER

DYSPROSIUM-ALUMINUM ALLOY FOILS IN WATER

Foil thickness		Faired experimental perturbation factor, F	Perturbation factor F^a			
τ_0	t, cm		No edge correction	Using Hanna's edge correction, ϵ_H	Using Tittle's edge correction, ϵ_T	Using surface to volume ratio correlation, S/V
0.01	0.024	0.96±0.03	0.956	0.962	0.964	0.957
.03	.072	.89± .03	.888	.906	.913	.893
.05	.120	.84± .03	.831	.856	.872	.842
.08	.192	.79± .02	.761	.804	.822	.785
.10	.240	.75± .02	.722	.769	.794	.752
.13	.312	.71± .02	.663	.723	.755	.704

[a]Calculated by Ritchie-Eldridge method.

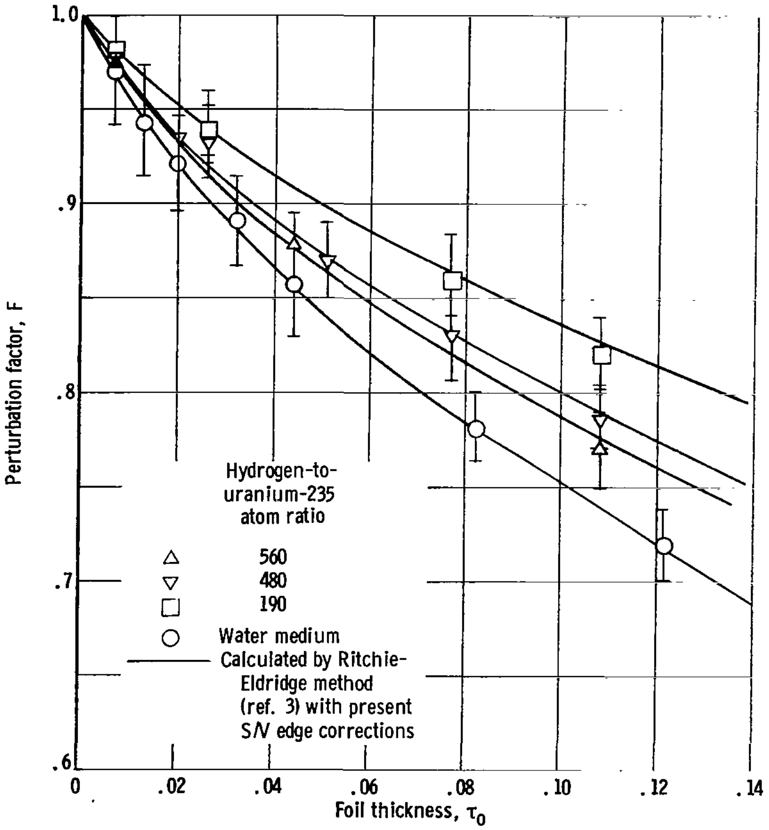

Figure 5. - Foil perturbation factors for 2.54-centimeter-diameter dyprosium-aluminum foils in water and uranyl fluoride - water solutions.

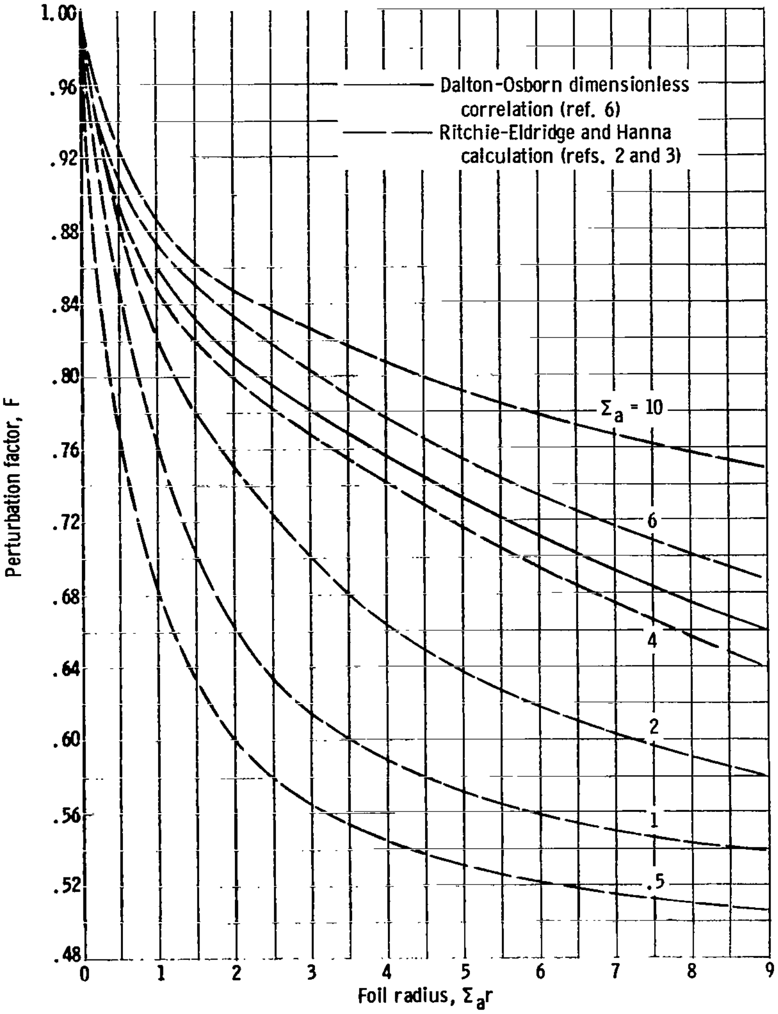

Figure 6. - Foil perturbation factors for coin-shaped foils of fixed optical thickness ($\Sigma_A t = 0.08$) in a water medium as function of dimensionless foil radius $\Sigma_a r$.

20 percent of the total foil surface so that these data should provide a test for the validity of edge corrections described earlier in equations (2) to (4). These corrections for water are indicated in figure 4 and listed in table II where the experimental perturbation factors faired from figure 4 are compared with the perturbation factor calculations.

The calculated perturbation factors containing an edge correction agree with the experimental values within the experimental uncertainty. However, the edge correction ϵ_T suggested by Tittle tends to overcorrect for the thicker foils.

It should be noted that the assigned experimental uncertainty shown in table II and figure 4 arises primarily from the uncertainty in the extrapolation to zero foil thickness and is applied uniformly as a function of τ_0. The agreement between the data and the calculations is consistent with the reported results for gold and indium foils in water as given in references 5, 7, and 10; however, the edge correction is a somewhat larger factor in the present calculations because of the relatively thick dysprosium-aluminum foils.

Also included in figure 4 are the generalized results of Dalton and Osborn (ref. 6) for disk-shaped detectors in water for which agreement is seen to be poor. It was necessary to extrapolate the Dalton-Osborn dimensionless plots to obtain values for the present dysprosium-aluminum foils which are out of the range of the dimensionless curves; however, the variation of foil perturbation factor with decreasing foil macroscopic cross section is clear in the Dalton-Osborn generalization which is believed to be limited in application. Inasmuch as the Dalton-Osborn and Ritchie-Eldridge and Hanna calculations had been compared by Hanna in reference 2 for a wide range of gold foil radii with good agreement, the source for the present disagreement for the dysprosium-aluminum foils has been investigated and is discussed in the section Generalized Dalton-Osborn Results.

Absorptive Diffusion Media

In figure 5, the experimental perturbation factors for water and for the uranyl fluoride - water solutions are plotted against τ_0. The curves are calculated using the Ritchie-Eldridge method and the present (S/V) edge correction. The calculations provide a good fit to the data for the uranyl fluoride - water solutions as well as for pure water. The calculated decrease in perturbation factor with increasing poison concentration is due primarily to the large change in diffusion length.

Generalized Dalton-Osborn Results

In studying their numerical calculations for coin-shaped gold detectors, Dalton and Osborn (ref. 6) found that the effects of scattering in gold foils on the perturbation factors were very small. Thus it appeared to them that for the sizes of detectors normally used, the important property of the detector was the absorption cross section. This probably suggested that the only important parameter required to generalize their results was the product of a detector dimension and its macroscopic absorption cross section. When the dimensionless parameter of detector absorption cross section times detector radius ($\Sigma_A r$) is used, the available experimental foil perturbation data for gold and indium coin-shaped detectors were fitted accurately by the same analytical set of curves. Generalized dimensionless plots of perturbation factors were prepared for coin-shaped detectors in graphite and water media. The correlation was indicated to be valid for a range of values of Σ_A from 1 to 10. The validity of the Dalton-Osborn generalization is simply tested by comparing calculated foil perturbation factors by the Dalton-Osborn method and by the Ritchie-Eldridge method and Hanna edge correction for a water medium containing coin-shaped foils of a fixed optical thickness but for a large range of Σ_A and the apparently general parameter $\Sigma_A r$. These results are presented in figure 6 for thickness $\Sigma_A t$ of 0.08, wherein by the Dalton-Osborn generalization, perturbation factors for materials with a range of Σ_A should lie on the single solid curve shown. However, a large spread in values results with assumed variations in Σ_A when calculated by the Ritchie-Eldridge method. It may be noted that the Dalton-Osborn curve coincides with a material of $\Sigma_A \approx 5$ and, therefore, correlates the foil perturbation data for gold ($\overline{\Sigma}_A = 5.5$) and for indium ($\overline{\Sigma}_A = 6.6$). However, the present data for dysprosium-aluminum with $\Sigma_A \approx 0.5$ are much lower than that predicted by Dalton and Osborn. The Ritchie-Eldridge calculation predicts that perturbation factors for foils of Σ_a greater than 6 or less than 4 are significantly different from the values obtained from the Dalton-Osborn generalization.

Lewis Research Center,
National Aeronautics and Space Administration,
Cleveland, Ohio, October 11, 1965.

REFERENCES

1. Osborn, R. K.: A Discussion of Theoretical Analyses of Probe-Induced Thermal Flux Perturbations. Nucl. Sci. Eng., vol. 15, no. 3, Mar. 1963, pp. 245-258.

2. Hanna, G. C.: The Neutron Flux Perturbation Due to an Absorbing Foil; A Comparison of Theories and Experiments. Nucl. Sci. Eng., vol. 15, no. 3, Mar. 1963, pp. 325-337.

3. Ritchie, R. H.; and Eldridge, H. B.: Thermal Neutron Flux Depression by Absorbing Foils. Nucl. Sci. Eng., vol. 8, no. 4, Oct. 1960, pp. 300-311.

4. Tittle, C. W.: Perturbation of Foil Activation in Thermal Neutron Fields. Trans. Am. Nucl. Soc., vol. 5, no. 1, June 1962, p. 33.

5. Walker, Jack V.; Randall, John D.; and Stinson, Ronald C., Jr.: Thermal Neutron Flux Perturbation Due to Indium Foils in Water. Nucl. Sci. Eng., vol. 15, no. 3, Mar. 1963, pp. 309-313.

6. Dalton, G. Ronald; and Osborn, Richard K.: Flux Perturbations by Thermal Neutron Detectors. Nucl. Sci. Eng., vol. 9, no. 2, Feb. 1961, pp. 198-210.

7. Zobel, W.: Experimental Determination of Corrections to the Neutron Activation of Gold Foils Exposed in Water. Rept. No. ORNL 3407, Oak Ridge Nat. Lab., Apr. 4, 1963.

8. Case, K. M.; deHoffmann, F.; and Placzek, G.: Introduction to the Theory of Neutron Diffusion. Vol. I. Los Alamos Sci. Lab., 1953, pp. 17-30.

9. Skyrme, T. H. R.: Reduction in Neutron Density Caused by an Absorbing Disc. Rept. No. MS 91, Second ed., British RAE, 1961.

10. Walker, J. V.: The Effects of Flux Anisotropy on Thermal-Neutron Flux Perturbations. Nucl. Sci. Eng., vol. 22, no. 1, May 1965, pp. 94-101.

11. Love, Bernard: Selection and Evaluation of Rare or Unusual Metals. Pt. II - The Metallurgy of Yttrium and the Rare Earth Metals. Rept. No. TR 57-666, WADC, Mar. 1959.

12. Beyster, J. R.; Wood, J. L.; Lopez, W. M.; and Walton, R. B.: Measurements of Neutron Spectra in Water, Polyethylene and Zirconium Hydride. Nucl. Sci. Eng., vol. 9, no. 2, Feb. 1961, pp. 168-184.

13. Starr, Eugene; and Koppel, Juan: Determination of Diffusion Hardening in Water. Nucl. Sci. Eng., vol. 14, no. 3, July 1962, pp. 224-229.

14. Sher, R.; Tassan, S.; Weinstock, E. V.; and Hellsten, A.: Low Energy Neutron Cross Sections of Dysprosium 164. Nucl. Sci. Eng., vol. 11, no. 4, Dec. 1961, pp. 369-376.

15. Hughes, Donald J.; and Schwartz, Robert B.: Neutron Cross Sections. Rept. No. BNL 325, Second ed., July 1, 1958.

NASA-Langley, 1966 E-3162

"The aeronautical and space activities of the United States shall be conducted so as to contribute . . . to the expansion of human knowledge of phenomena in the atmosphere and space. The Administration shall provide for the widest practicable and appropriate dissemination of information concerning its activities and the results thereof."

—NATIONAL AERONAUTICS AND SPACE ACT OF 1958

NASA SCIENTIFIC AND TECHNICAL PUBLICATIONS

TECHNICAL REPORTS: Scientific and technical information considered important, complete, and a lasting contribution to existing knowledge.

TECHNICAL NOTES: Information less broad in scope but nevertheless of importance as a contribution to existing knowledge.

TECHNICAL MEMORANDUMS: Information receiving limited distribution because of preliminary data, security classification, or other reasons.

CONTRACTOR REPORTS: Technical information generated in connection with a NASA contract or grant and released under NASA auspices.

TECHNICAL TRANSLATIONS: Information published in a foreign language considered to merit NASA distribution in English.

TECHNICAL REPRINTS: Information derived from NASA activities and initially published in the form of journal articles.

SPECIAL PUBLICATIONS: Information derived from or of value to NASA activities but not necessarily reporting the results of individual NASA-programmed scientific efforts. Publications include conference proceedings, monographs, data compilations, handbooks, sourcebooks, and special bibliographies.

Details on the availability of these publications may be obtained from:

SCIENTIFIC AND TECHNICAL INFORMATION DIVISION
NATIONAL AERONAUTICS AND SPACE ADMINISTRATION
Washington, D.C. 20546